STATISTICAL LONG TERM CREEP FAILURE TIME OF UNIDIRECTIONAL CFRP

Yasushi Miyano[1] and Masayuki Nakada[2]

[1, 2] Materials System Research Laboratory, Kanazawa Institute of Technology
3-1 Yatsukaho Hakusan Ishikawa 924-0838, Japan
miyano@neptune.kanazawa-it.ac.jp
nakada@neptune.kanazawa-it.ac.jp

Keywords: CFRP, Viscoelasticity, Life prediction, Tensile strength, Creep failure time

ABSTRACT

A method for statistical prediction of the long-term creep failure time of CFRP using the statistical static strengths of CFRP at various temperatures and the viscoelasticity of matrix resin is proposed based on Christensen's model of viscoelastic crack kinetics. The tensile strength along the longitudinal direction of unidirectional CFRP constitutes important data for the reliable design of CFRP structures. The authors developed a reliable method for testing creep and fatigue strengths as well as static strength at elevated temperatures for resin-impregnated carbon fiber strands (CFRP strands) as unidirectional CFRP. Two kinds of CFRP strands with two types of PAN-based carbon fibers were examined in this study. The statistical static strengths of these CFRP strands and the creep compliances of matrix resins were measured at various temperatures. The tensile creep failure times of these CFRP strands are predicted statistically based on a prediction method using measured data. The predicted creep failure times of these CFRP strands were compared with the creep failure times of these CFRP strands measured experimentally and statistically.

1 INTRODUCTION

Carbon fiber reinforced plastics (CFRP) have been used for primary structures of airplanes, ships, automobiles, and other vehicles for which high reliability must be maintained during long-term operation. Therefore, an accelerated testing methodology is strongly anticipated for the long-term life prediction of CFRP structures exposed to actual environmental temperatures, water, and other influences.

The mechanical behavior of matrix resin of CFRP exhibits time and temperature dependence, called viscoelastic behavior, not only above the glass transition temperature T_g, but also below T_g. Consequently, it can be inferred that the mechanical behavior of CFRP depends strongly on time and temperature [1–5]. Our earlier reports have proposed the formulation of statistical static, creep, and fatigue strengths of CFRP based on matrix resin viscoelasticity [6–7].

The tensile strength along the longitudinal direction of unidirectional CFRP constitutes important data for the reliable design of CFRP structures. The authors developed a reliable test method to assess creep and fatigue strengths, as well as the static strength, at elevated temperatures for resin-impregnated carbon fiber strands (CFRP strands) combined with PAN based high strength carbon fibers T300-3000 and epoxy resin [8]. Furthermore, the authors confirmed that the time-dependent and temperature-dependent tensile static strength is controlled by the viscoelastic behavior of matrix resin based on the Rosen's shear lag model [9]. Additionally, the authors developed a test method for the CFRP strand of more high strength carbon fibers T800-12000 and epoxy resin with a highly reliable co-cured tab. The temperature-dependent tensile strength of this CFRP strand was evaluated [10].

Our most recent study undertook the prediction of statistical creep failure time under tension loading along the longitudinal direction of unidirectional CFRP performed using CFRP strands of two kinds of high strength carbon fibers T800-12000 and T300-3000, and epoxy resin [11, 12]. The statistical creep failure time of these CFRP strands at a constant load and temperature was predicted using statistical results of static tensile strengths of CFRP strands measured at various temperatures,

and the viscoelastic behavior of matrix resin. The predicted results statistically agreed well with the experimentally obtained results measured using creep tests for these CFRP strands.

For this study, the proposed method of predicting the statistical creep failure time under the tension loading along the longitudinal direction of unidirectional CFRP from the statistical static strengths of unidirectional CFRP measured at various temperatures is applied to various unidirectional CFRP with carbon fibers of different kinds. First, the method of predicting the statistical creep failure time of CFRP from the statistical static strengths of CFRP measured at various temperatures is proposed again based on Christensen's model of viscoelastic crack kinetics [13]. Second, two kinds of CFRP strands with PAN-based high strength and high modulus carbon fibers were prepared as specimens for unidirectional CFRP. Third, the static strengths of these CFRP strands were measured experimentally and statistically at various temperatures. Then the creep failure times of these CFRP strands were predicted statistically using the statistical static strengths based on the predictive method. Finally, the creep failure times of these CFRP strands at several constant loads and a temperature were measured experimentally and probabilistically using these CFRP strands for comparison with the predicted ones. Furthermore, the difference of time and temperature dependence on the static and creep strengths for two kinds of CFRP strands are discussed with the fractographs of these CFRP strands.

2 STATISTICAL PREDICTION OF CREEP FAILURE TIME OF CFRP

We have proposed the formulation for the statistical static strength σ_s of CFRP based on the viscoelasticity of matrix resin, as shown in the following equation in our previous paper [7]:

$$\log \sigma_s(P_f, t, T) = \log \sigma_0(t_0, T_0) + \frac{1}{\alpha_s} \log[-\ln(1-P_f)] - n_R \log\left[\frac{D^*(t,T)}{D_c(t_0,T_0)}\right], \quad (1)$$

where P_f signifies the failure probability, t denotes the failure time, t_0 represents the reference time, T is the temperature, T_0 stands for the reference temperature, σ_0 and α_s respectively denote the scale parameter and the shape parameter on the Weibull distribution of static strength, n_R is the viscoelastic parameter, and D_c and D^* respectively represent the creep and viscoelastic compliances of matrix resin. The viscoelastic compliance D^* for the static load with a constant strain rate is shown as

$$D^*(t,T) = D_c(t/2, T). \quad (2)$$

The statistical static strength σ_s is shown by the following equation by substituting Equation (2) into Equation (1).

$$\log \sigma_s(P_f, t, T) = \log \sigma_0(t_0, T_0) + \frac{1}{\alpha_s} \log[-\ln(1-P_f)] - n_R \log\left[\frac{D_c(t/2,T)}{D_c(t_0,T_0)}\right] \quad (3)$$

The relation between the creep failure time and the static failure time can be shown by Figure 1 [11]. This figure shows the creep strength and the static strength versus the failure time. The creep strength curve is obtainable by horizontally shifting the static strength curve by the amount log A. Therefore, the statistical creep strength σ_c is shown by the following equation.

$$\log \sigma_c(P_f, t, T) = \log \sigma_0(t_0, T_0) + \frac{1}{\alpha_s} \log[-\ln(1-P_f)] - n_R \log\left[\frac{D_c(At/2,T)}{D_c(t_0,T_0)}\right] \quad (4)$$

The failure probability of CFRP under a constant creep stress σ_{c0} can be shown by the following equation from Equation (4).

$$P_f = 1 - \exp(-F),\ \log F = \alpha_s \log\left[\frac{\sigma_{c0}}{\sigma_0}\right] + \alpha_s n_R \log\left[\frac{D_c(At/2,T_0)}{D_c(t_0,T_0)}\right] \quad (5)$$

The shifting amount log A is determined by the slope k_R of the static strength curve shown in Figure 1 as

$$\log A = \log(1+1/k_R), \qquad k_R = n_R m_R \tag{6}$$

where n_R is the viscoelastic parameter in Equations (1) and (3), and where m_R is the slope of logarithmic creep compliance of matrix resin against the logarithmic time [11,12].

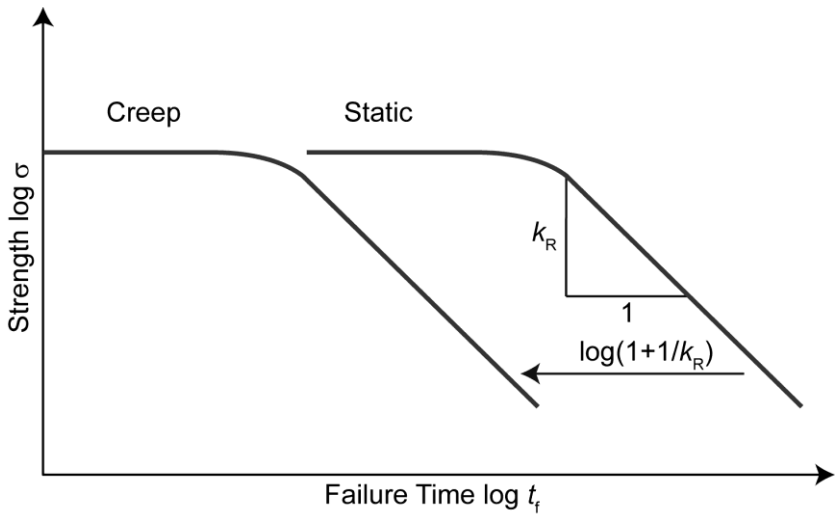

Figure 1: Time shifting between static strength and creep strength [11, 12].

3 MOLDING OF CFRP STRANDS

Two kinds of PAN-based carbon fibers of two kinds were prepared in this study, as shown in Table 1. PAN-based carbon fibers are high-strength type carbon fiber T300-3000 and high modulus type carbon fiber M40J-6000 (Toray Industries Inc.). Weibull distributions of the static strengths σ_c for carbon fibers of two kinds with shape parameters α_c and scale parameters β_c are shown in Figure 2.

Two CFRP strands with carbon fibers of two kinds and a general purpose epoxy resin jER828 (Mitsubishi Chemical Corp.) were molded using a filament winding system developed by the authors [8]. Actually, 200 specimens for two kinds of CFRP strands are molded, respectively, at one time using this system. Table 2 presents a composition of epoxy resin and the cure condition of CFRP strand. The gage lengths of CFRP strands are approximately 200 mm. The glass transition temperatures T_g = 160°C of the epoxy resin are determined from the peak of loss tangent against temperature at 1 Hz using the DMA test. The fiber volume fraction V_f = 55% of CFRP strand is ascertained from the weight of CFRP strands.

Table 1 Carbon fibers used in this study and mechanical properties by catalogs

Name	Density [g/cm^3]	Tex [g/km]	Elastic modulus [MPa]	Tensile Strength [MPa]
T300-3000	1.76	198	230	3530
M40J-6000	1.75	225	377	4400

Table 2 Composition and cure schedule of CFRP strand

CFRP strand	Carbon fiber	Composition of resin (weight ratio)	Cure schedule
T300/EP	T300-3000	Epoxy: jER828 (100) Hardener: MHAC-P (103.6) Cure accelerator: 2E4MZ (1)	70°C × 12 h + 150°C × 4 h + 190°C × 2 h
M40J/EP	M40J-6000		

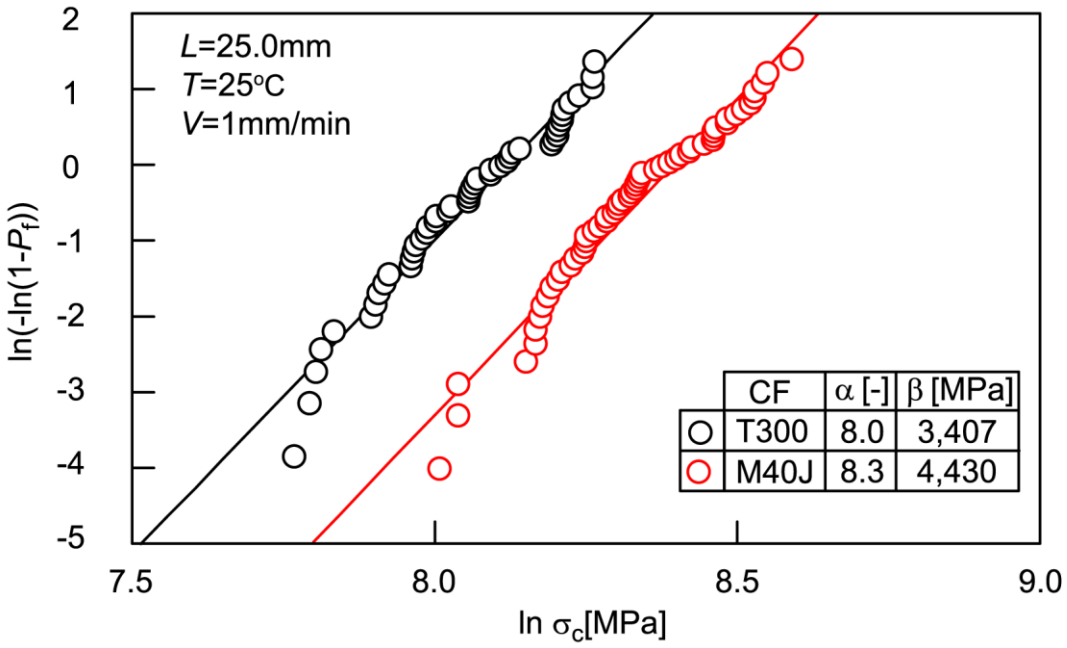

Figure 2 Weibull distributions of static strengths of single fibers of two kinds.

4 CREEP COMPLIANCE OF MATRIX RESIN

The dimensionless creep compliance D_c/D_{c0} measured at various temperatures is shown at the left of Figure 5. Long-term D_c/D_{c0} at T=120°C was obtained by horizontally shifting those at various temperatures, as shown at the right of Figure 3 [11, 12]. The reference temperature and time were selected as T_0=25°C and t_0=1 min in this study. The creep compliance at reference temperature and reference time D_{c0} was 0.33 GPa^{-1}. The dashed curve is the dimensionless viscoelastic compliance D^* of the matrix resin under the constant strain rate at T=120°C. The maximum slope in this figure is m_R = 0.28 shown in Equation (6).

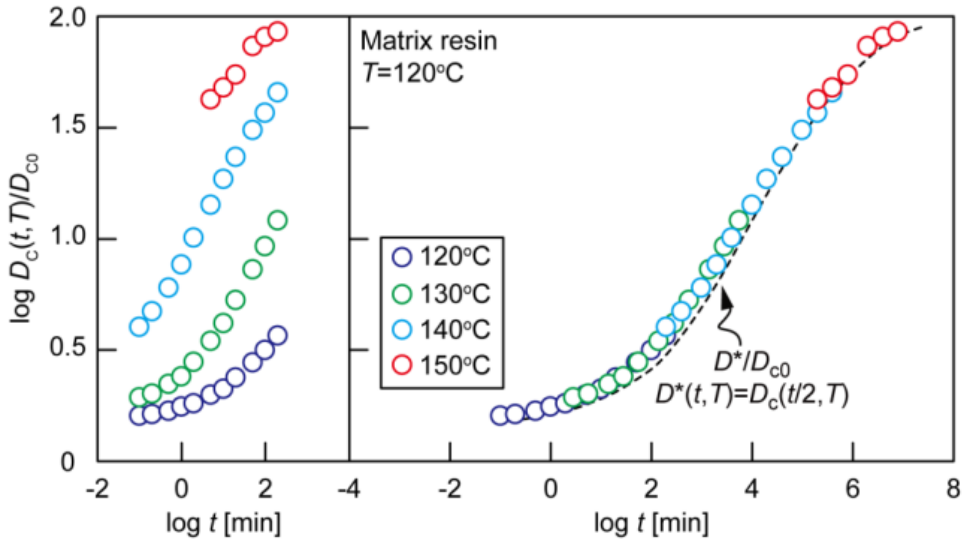

Figure 3. Dimensionless creep compliance of matrix resin at T=120°C [11, 12].

5 STATIC STRENGTHS OF CFRP STRANDS

The static tension tests for two kinds of CFRP strands T300/EP and M40J/EP with PAN-based carbon fibers were conducted at four or three temperature levels, 25°C, 135°C, 150°C and 170°C with

2 mm/min cross-head speed. The tensile strength of the CFRP strand σ_s was obtained using the following equation.

$$\sigma_s = \frac{P_{max}}{t_e}\rho \tag{7}$$

Therein, P_{max} stands for the maximum load [N]. ρ and t_e respectively represent the density of carbon fiber [kg/m^3] and the tex of a carbon fiber strand [g/1000 m].

Figure 4 presents static strengths versus temperature for CFRP strands of two kinds: T300/EP and M40J/EP. The Weibull distributions for the static strength of CFRP strand T300/EP at three temperatures are shown in Figure 5, where α_s is the shape parameter and β_s is the scale parameter of CFRP strand. Although the scale parameter decreases according to the temperature rise, the shape parameter maintains an almost constant value. Figure 6 is the Weibull distribution for the static strength of M40J/EP at four temperatures. Scale parameter β_s maintains almost a constant value below the temperature T=150°C and decreases drastically over T=150°C although the shape parameter α_s maintain almost a constant value for all temperatures in the case of M40J/EP.

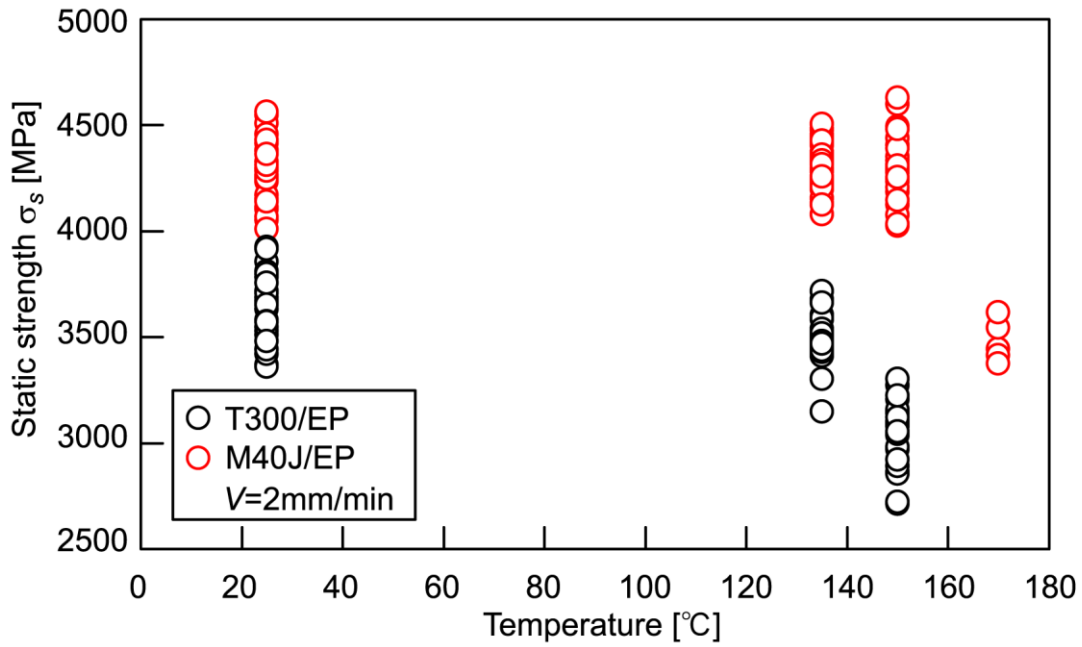

Figure 4. Static strength of T300/EP and M40/EP versus temperature.

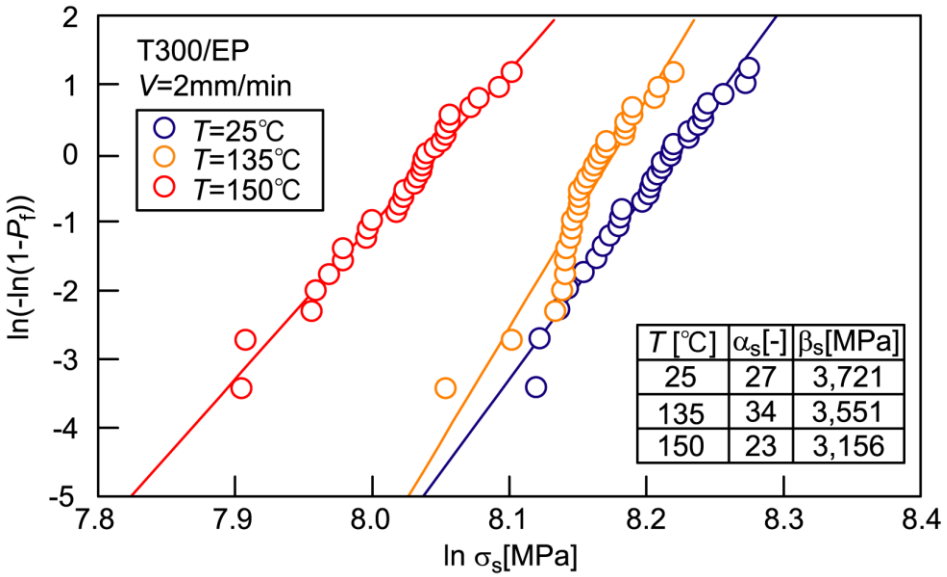

Figure 5. Weibull distributions of static tensile strength of T300/EP at four temperatures.

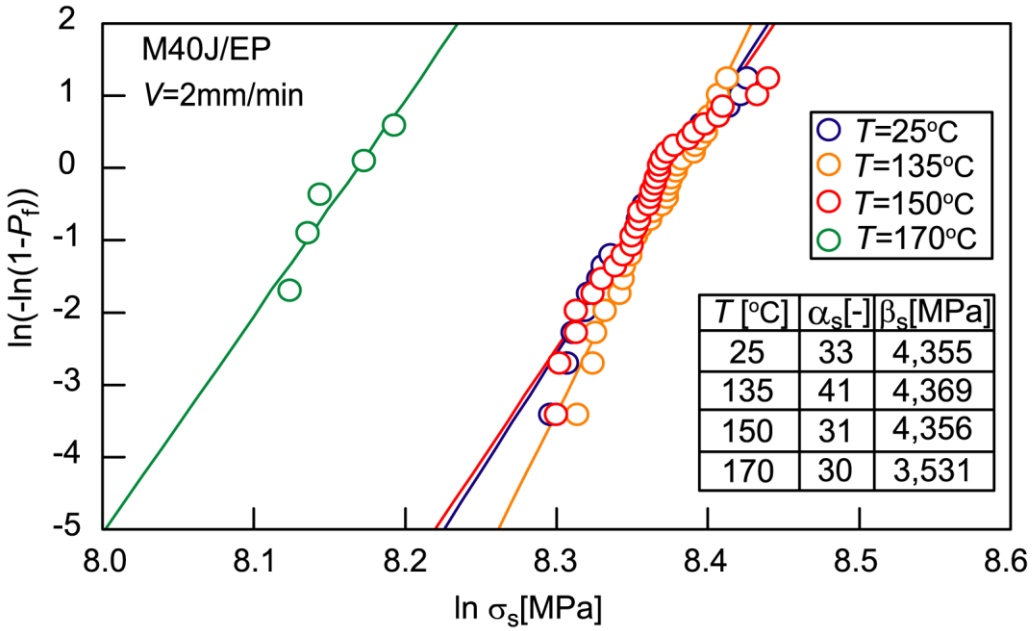

Figure 6. Weibull distributions of static tensile strength of M40J/EP at three temperatures.

6 DETERMINATION OF VISCOELASTIC PARAMETERS

Figures 7 and 8 show the dimensionless static strength σ_s/σ_0 against the dimensionless viscoelastic compliance of matrix resin D^*/D_{c0} simultaneously and temperature for T300/EP and M40J/EP. The relation of σ_s/σ_0 against D^*/D_{c0} can be shown by one or two straight lines with the slope of n_R, which is the viscoelastic parameter in Equations (1), (3), and (5). The slopes of both CFRP strands are completely different from one another.

All parameters in Equations (1), (3), and (5) were determined by measuring the creep compliance of matrix resin and the statistical static strength of CFRP strand at various temperatures through the above process. They are shown in Table 3.

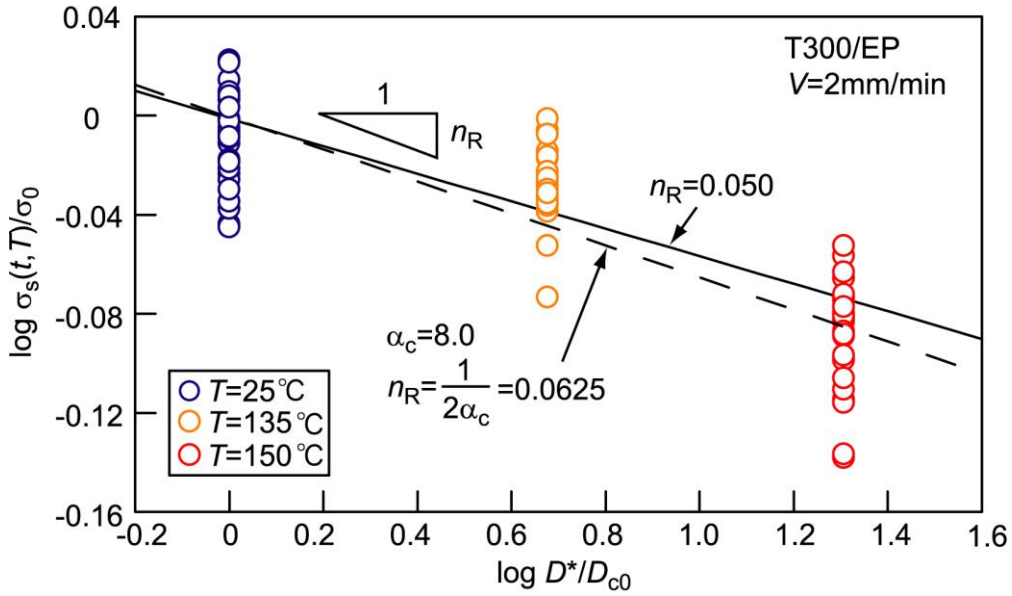

Figure 7. Static strength of T300/EP against viscoelastic compliance of matrix resin.

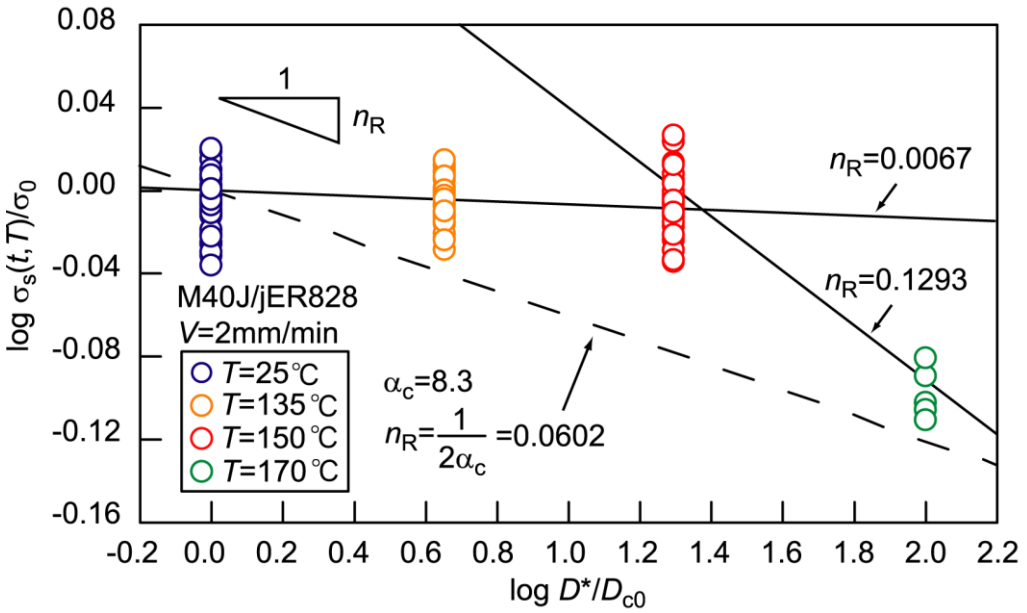

Figure 8. Static strength of M40J/EP against viscoelastic compliance of matrix resin.

Table 3. Parameters for statistical creep failure time prediction

Parameters	T300/EP	M40J/EP	M40J/EP
σ_0 [MPa]	3,721	4,355	(6418)
α_s	27	33	33
n_R	0.050	0.0067	0.1293
m_R	0.28	0.28	0.28
k_R	0.014	0.00188	0.0362
log A	1.86	2.73	1.46

7 CREEP FAILURE TIME OF CFRP STRANDS

Creep failure tests of T300/EP and M40J/EP were conducted using a specially designed creep failure testing machine [11]. The test conditions are presented in Table 4. Results of the creep failure tests are presented in Figures 9 and 10. The predicted creep failure probability against failure time calculated by substituting the parameters of Table 3 into Equations (5) and (6) is also shown in Figures 9 and 10. The predicted statistical creep failure time agrees well with the experimental data for both of T300/EP and M40J/EP although the viscoelastic parameter n_R for T300/EP is a constant in the range of all temperatures as shown in Figure 7 and the n_R for M40J/EP changes drastically by temperatures as shown in Figure 8.

Table 4. Conditions of creep failure tests for CFRP strands

CFRP strand	Temperature T (°C)	Creep stress σ_{c0} (MPa)	σ_{c0}/σ_0 (%)	Number of specimens
T300/EP	120	3,126	84	20
		3,312	89	20
		3,498	94	20
M40J/EP	120	3,658	84	20
		3,876	89	20
		4,094	94	20

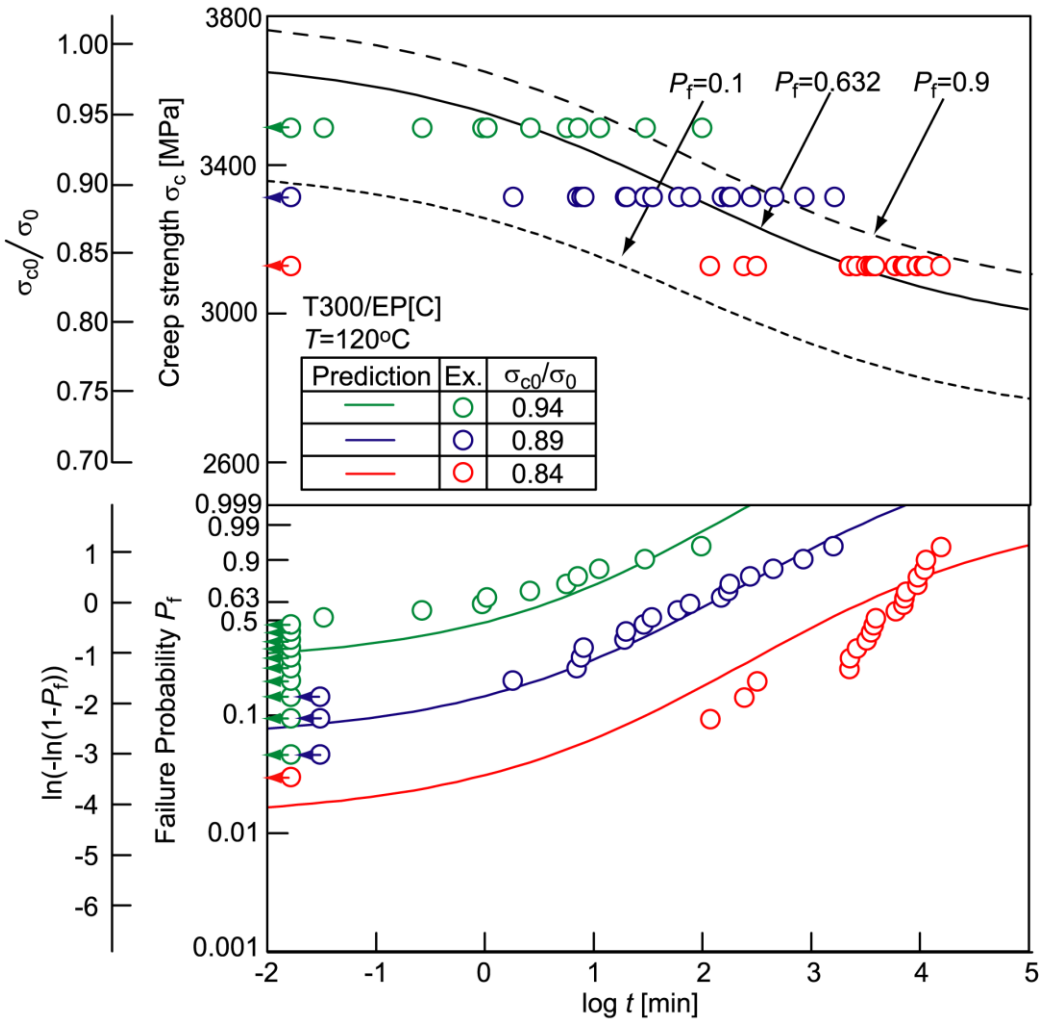

Figure 9. Failure probability against creep failure time of T300/EP.

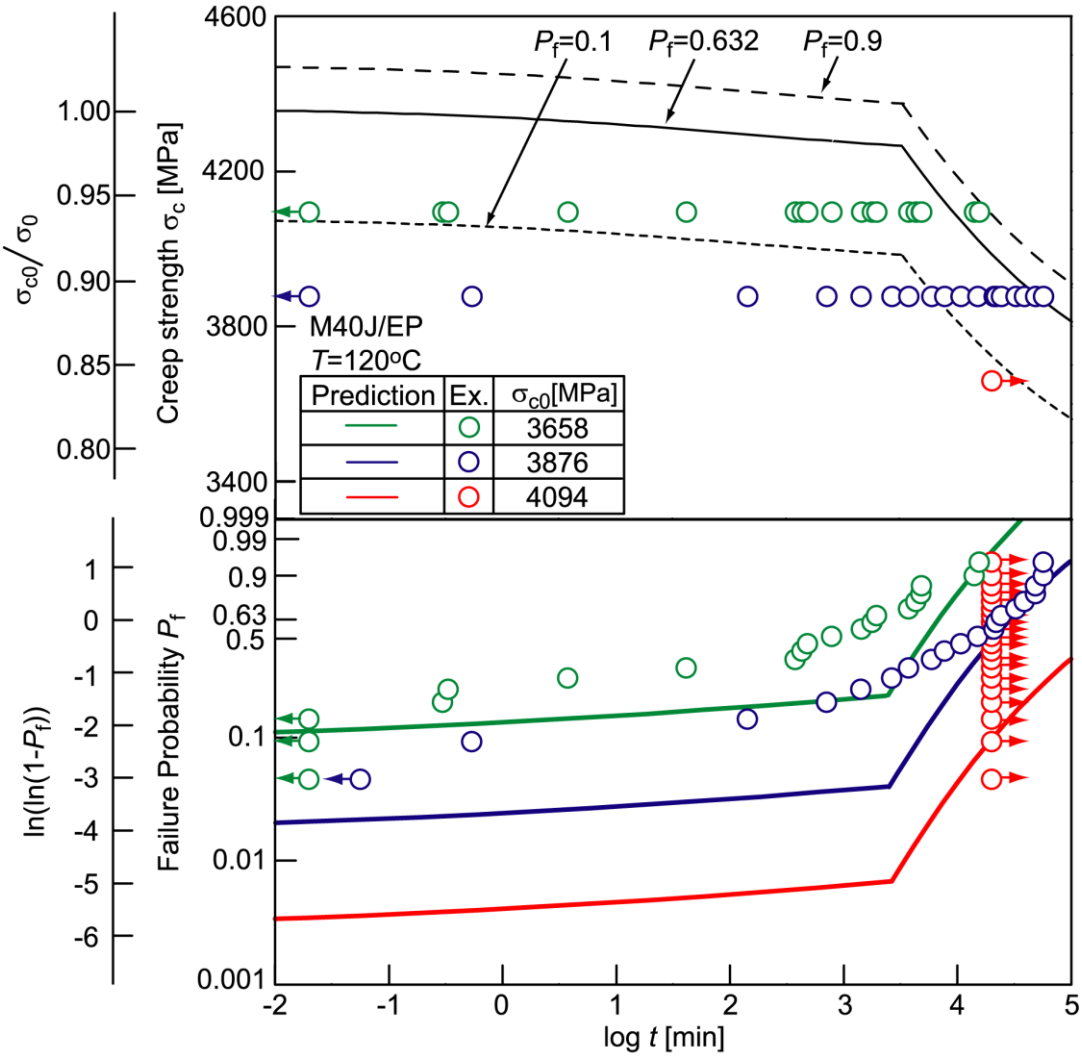

Figure 10. Failure probability against creep failure time of M40/EP.

8 FRACTOGRAPHS AFTER STATIC AND CREEP TESTS

Figures 11 and 12 respectively portray fractographs of T300/EP and M40J/EP after the static tests and creep tests. These figures clarify that the fractures of CFRP strands show different tendencies. A markedly uneven failure surface is observed in all conditions of static and creep tests for T300/EP, where penetrations of cracks through fibers are not observed. However, a mirror surface with a wide area is observed in the conditions of low temperature and short time of static and creep tests for M40J/EP, where the generated cracks penetrate through numerous fibers, although uneven failure surface is observed in the conditions of high temperature and long time of static and creep tests. These behavior of fractographs for both CFRP strands are corresponding well with these behavior of viscoelastic parameters n_R for both CFRP strands.

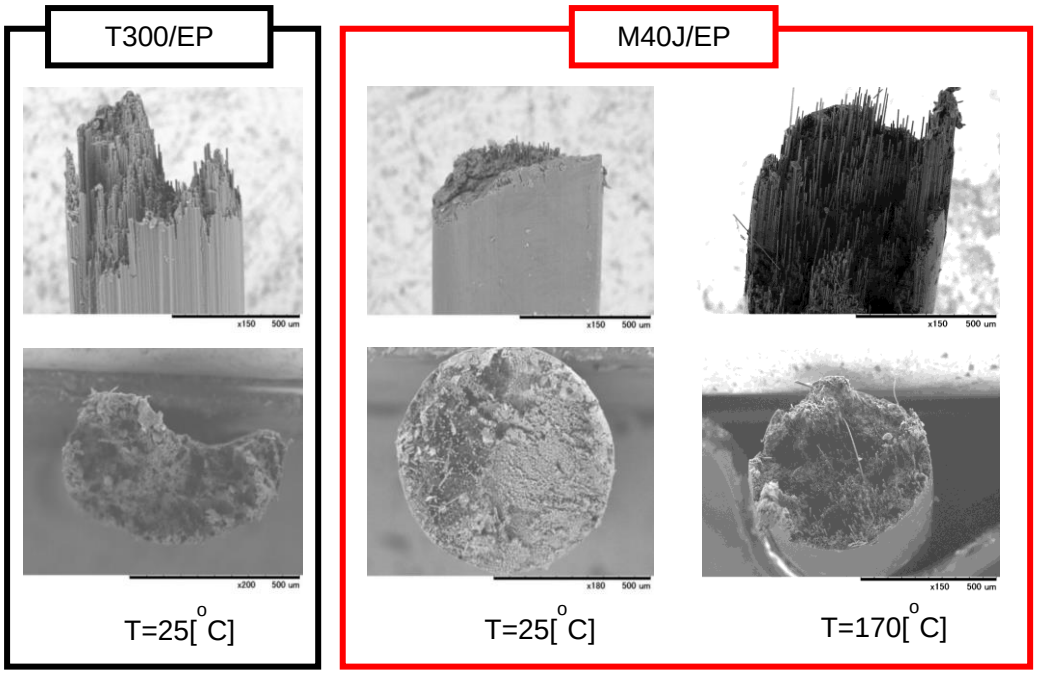

Figure 11. Fractographs of T300/EP and M40J/EP after static tension tests.

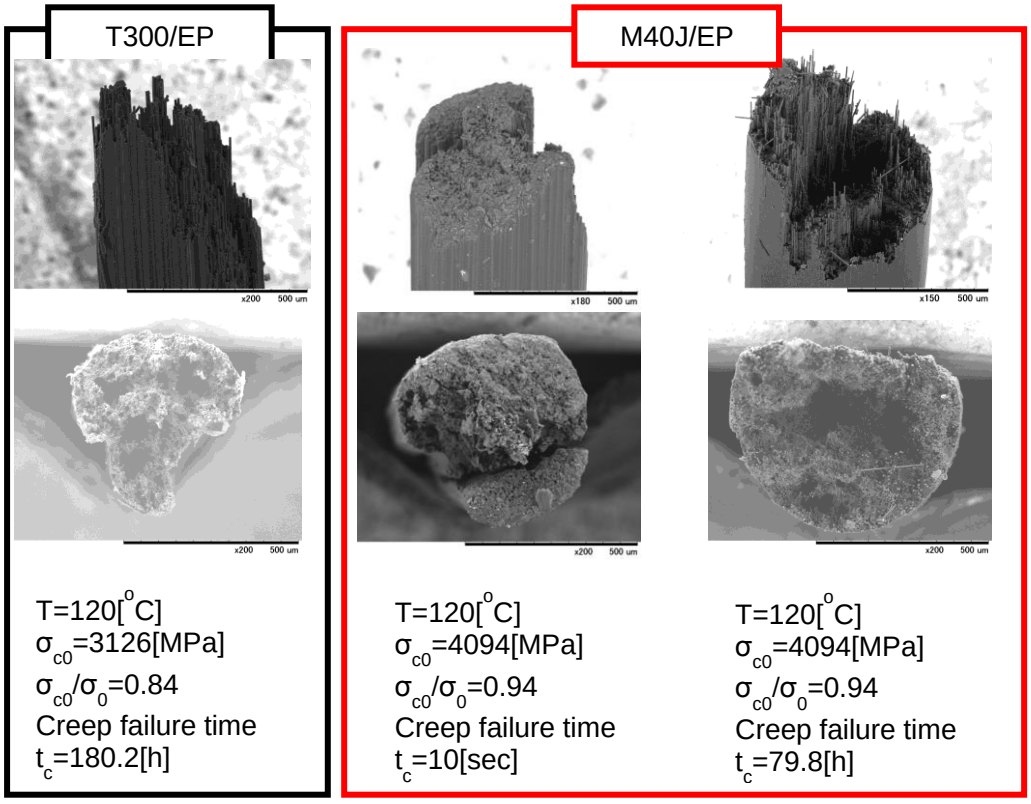

Figure 12. Fractographs of T300/EP and M40J/EP after creep tests

.

9 DISCUSSING OF FAILURE MECHANISMS

The experimental viscoelastic parameters n_R for T300/EP as shown in Figure 7 agree with the theoretical viscoelastic parameters n_R determined from $n_R = 1/2\alpha_c$ based on Rosen's shear lag model[11], where α_c is the shape parameter for tensile strength of single carbon fiber shown on Figure 2. Therefore, it can be presumed that the failure mechanism of T300/EP is based on Rosen's shear lag model. The failure of a carbon fiber based on Rosen's shear lag model is not influenced from other carbon fibers and therefore the markedly uneven failure surface should be observed on the fractograph of CFRP strand. Actually, the fractographs of T300/EP show the uneven failure surfaces as shown in Figures 11 and 12.

On the other hand, the failure of M40J/EP shows brittle fracture in the range of low temperature and short time as shown in these figures, and the static and creep strengths of this CFRP strand do not show time and temperature dependent behavior and the viscoelastic parameters n_R are nearly equal to zero in this range. In the range of high temperature and long time, M40J/EP shows the markedly uneven failure surface, and the static and creep strengths of this CFRP strand show remarkably time and temperature dependent behavior and the viscoelastic parameter n_R trends to that for Rosen's shear lag model.

10 CONCLUSIONS

We proposed a prediction method for statistical creep failure time under tension loading along the longitudinal direction of unidirectional CFRP using the statistical static tensile strength of CFRP strand and the viscoelasticity of matrix resin based on Christensen's model for viscoelastic crack kinetics. Results clarified that this prediction method is applicable for CFRP strands with PAN-based carbon fibers.

Statistical considerations related to strength should be associated strongly with the size effect of strength, as discussed in our recent paper [14]. Through these discussions, our results for resin impregnated CFRP strands shall be extended in future studies to general CFRP structures that must have high reliability.

Statistical considerations related to the strength should be also associated with the water effect of strength for marine use. Our proposed methodology shall be useful for these discussions.

ACKNOWLEDGEMENTS

The authors thank the Office of Naval Research for supporting this work through an ONR award to Dr. Yapa Rajapakse and Dr. Ming-Jen Pan. Our award, "Statistical Long Term Creep Failure Time of Unidirectional CFRP," is numbered N62909-16-1-2132. The authors thank Professor Richard Christensen of Stanford University as a partner on this project.

REFERENCES

1. J. Aboudi, G., Cederbaum, "Analysis of Viscoelastic Laminated Composite Plates", *Composite Structures*; 12: 243–256, 1989
2. J. Sullivan, "Creep and Physical Aging of Composites", *Composite Science and Technology*; 39: 207–232, 1990
3. T. Gates, "Experimental Characterization of Nonlinear, Rate Dependent Behavior in Advanced Polymer Matrix Composites", *Experimental Mechanics*; 32: 68–73, 1992

4. Y. Miyano, M. Nakada, M. K. McMurray, R. Muki, “Prediction of Flexural Fatigue Strength of CFRP Composites under Arbitrary Frequency, Stress Ratio and Temperature”, *Journal of Composite Materials*; 31: 619–638, 1997
5. M. Kawai, Y. Yagihashi, H. Hoshi, Y. Iwahori, “Anisomorphic Constant Fatigue Life Diagrams for Quasi-isotropic Woven Fabric Carbon/epoxy Laminates under Different Hygro-thermal Environments”, *Advanced Composite Materials*; 22: 79–98, 2013
6. Y. Miyano, M. Nakada, H. Cai, “Formulation of Long-term Creep and Fatigue Strengths of Polymer Composites Based on Accelerated Testing Methodology”, *Journal of Composite Materials*; 42: 1897–1919, 2008
7. M. Nakada, Y. Miyano, “Advanced Accelerated Testing Methodology for Long-Term Life Prediction of CFRP Laminates”, *Journal of Composite Materials*; 49: 163–175, 2015
8. Y. Miyano, M. Nakada, H. Kudoh, R. Muki, “Prediction of Tensile Fatigue Life under Temperature Environment for Unidirectional CFRP”, *Advanced Composite Materials*; 8: 235–246, 1999
9. M. Nakada, Y. Miyano, M. Kinoshita, R. Koga, T. Okuya, R. Muki, “Time-Temperature Dependence of Tensile Strength of Unidirectional CFRP”, *Journal of Composite Materials*; 36: 2567–2581, 2002
10. T. Okuya, M. Nakada, Y. Miyano, “Reliable Test Method for Tensile Strength in Longitudinal Direction of Unidirectional Carbon Fiber-Reinforced Plastics”, *Journal of Reinforced Plastics and Composites*; 32: 1579–1585, 2013
11. M. Nakada, T. Okuya, Y. Miyano, “Statistical Prediction of Tensile Creep Failure Time for Unidirectional CFRP”, *Advanced Composite Materials*; 23: 451–460, 2014
12. M. Nakada, Y. Miyano, “Statistical Creep Failure Time of Unidirectional CFRP”, Experimental Mechanics; 56: 653-658, 2016
13. R. Christensen, Y. Miyano, “Stress Intensity Controlled Kinetic Crack Growth and Stress History Dependent Life Prediction with Statistical Variability”, *International Journal of Fracture*; 137: 77–87, 2006
14. R. Christensen, Y. Miyano, M. Nakada, “Size Dependence of Tensile Strength for Brittle Isotropic Materials and Carbon Fiber Composite Materials”, *Composites Science and Technology*; 106: 9–14, 2015